Reprinted from

MARINE CHEMISTRY

AN INTERNATIONAL JOURNAL FOR STUDIES OF THE MARINE ENVIRONMENT

Marine Chemistry 68 (2000) 183–201

A seasonal tropical sink for atmospheric CO_2 in the Atlantic ocean: the role of the Amazon River discharge

J.F. Ternon [a], C. Oudot [b,*], A. Dessier [b], D. Diverres [b]

[a] *IRD, Cayenne, French Guiana*
[b] *IRD, Brest, France*

Received 15 March 1999; received in revised form 19 July 1999; accepted 20 July 1999

MARINE CHEMISTRY

Scope of the journal
Marine Chemistry is an international medium for the publication of original studies and occasional reviews in the field of chemistry in the marine environment, with emphasis on the dynamic approach. The journal will endeavour to cover all aspects, from chemical processes to theoretical and experimental work, and, by providing a central channel of communication, to speed the flow of information in this relatively new and rapidly expanding discipline.

Publication information
Marine Chemistry (ISSN 0304-4203). For 2000, volumes 68–72 are scheduled for publication. Subscription prices are available upon request from the Publisher or from the Regional Sales Office nearest you or from this journal's website (http://www.elsevier.nl/locate/marchem). Further information is available on this journal and other Elsevier Science products through Elsevier's website: (http://www.elsevier.nl). Subscriptions are accepted on a prepaid basis only and are entered on a calendar year basis. Issues are sent by standard mail (surface within Europe, air delivery outside Europe). Priority rates are available upon request. Claims for missing issues should be made within six months of the date of dispatch.

Orders, claims, and product enquiries: please contact the Customer Support Department at the Regional Sales Office nearest you:
New York: Elsevier Science, PO Box 945, New York, NY 10159-0945, USA; phone: (+1) 212 633 3730 [toll free number for North American customers: 1-888-4ES-INFO (437-4636)]; fax: (+1) 212 633 3680; e-mail: usinfo-f@elsevier.com
Amsterdam: Elsevier Science, PO Box 211, 1000 AE Amsterdam, The Netherlands; phone: (+31) 20 4853757; fax: (+31) 20 4853432; e-mail: nlinfo-f@elsevier.nl
Tokyo: Elsevier Science, 9-15 Higashi-Azabu 1-chome, Minato-ku, Tokyo 106-0044, Japan; phone: (+81) (3) 5561 5033; fax: (+81) (3) 5561 5047; e-mail: info@elsevier.co.jp
Singapore: Elsevier Science, No. 1 Temasek Avenue, #17-01 Millenia Tower, Singapore 039192; phone: (+65) 434 3727; fax: (+65) 337 2230; e-mail: asiainfo@elsevier.com.sg
Rio de Janeiro: Elsevier Science, Rua Sete de Setembro 111/16 Andar, 20050-002 Centro, Rio de Janeiro - RJ, Brazil; phone: (+55) (21) 509 5340; fax: (+55) (21) 507 1991; e-mail: elsevier@campus.com.br [Note (Latin America): for orders, claims and help desk information, please contact the Regional Sales Office in New York as listed above].

Advertising information. Advertising orders and enquiries can be sent to: **USA, Canada and South America:** Mr Tino de Carlo, The Advertising Department, Elsevier Science Inc., 655 Avenue of the Americas, New York, NY 10010-5107, USA; Tel.: (+1) (212) 633 3815; fax: (+1) (212) 633 3820; e-mail: t.decarlo@elsevier.com. **Japan:** The Advertising Department, Elsevier Science K.K., 9-15 Higashi-Azabu 1-chome, Minato-ku, Tokyo 106-0044, Japan; Tel.: (+81) (3) 5561-5033; fax: (+81) (3) 5561 5047. **Europe and ROW:** Rachel Leveson-Gower, The Advertising Department, Elsevier Science Ltd., The Boulevard, Langford Lane, Kidlington, Oxford OX5 1GB, UK; Tel.: (+44) (1865) 843565; fax: (+44) (1865) 843976; e-mail: r.leveson-gower@elsevier.co.uk.

♾ The paper used in this publication meets the requirements of ANSI/NISO Z39.48-1992 (Permanence of Paper).

PRINTED IN THE NETHERLANDS

ELSEVIER

Marine Chemistry 68 (2000) 183–201

MARINE CHEMISTRY

www.elsevier.nl/locate/marchem

A seasonal tropical sink for atmospheric CO_2 in the Atlantic ocean: the role of the Amazon River discharge

J.F. Ternon [a], C. Oudot [b,*], A. Dessier [b], D. Diverres [b]

[a] *IRD, Cayenne, French Guiana*
[b] *IRD, Brest, France*

Received 15 March 1999; received in revised form 19 July 1999; accepted 20 July 1999

Abstract

In the western equatorial Atlantic ocean, near-surface observations show that during summertime, the low-salinity oceanic water, arising from mixing with the Amazon River discharge at the equator, has low CO_2 fugacity levels. Near the coast of South America where the salinities are the lowest ($S < 20$), the fugacity of oceanic CO_2 decreases down to 150 μatm and the shelf area acts as a significant sink for atmospheric CO_2. The dilution effect by low-salinity water only partly accounts for the decrease in CO_2, and the biological production in the Amazon Plume water enriched in nutrients lowers dissolved inorganic carbon and decreases the fCO_2 by nearly 30%. The low-salinity Amazon water tongue spreads northwestwards along the coast by the North Brazil Current (NBC) and is deflected eastwards north of 5°N in the NBC retroflection in summer. Consequently, the low-salinity and oceanic fCO_2 (below the atmospheric fCO_2 level) signatures may extend more than 2000 km eastwards. The impact of the river outflow on the air–sea CO_2 exchanges in the western region is demonstrated by using the climatologies of the sea surface salinity (SSS) to estimate the magnitude of the annual net CO_2 flux in the western part of the equatorial Atlantic. This is in contrast with the central and eastern parts that are sources for atmospheric CO_2.

Keywords: surface seawater; fCO_2; salinity; CO_2 flux; sink; river; productivity

1. Introduction

The Atlantic equatorial belt (10°N–10°S) is generally regarded as an oceanic source of CO_2 for the atmosphere (Keeling and Waterman, 1968; Takahashi et al., 1978; Roos and Gravenhorst, 1984; Smethie et al., 1985; Andrié et al., 1986; Oudot et al., 1987; Oudot et al., 1995; Schneider and Morlang, 1995; Goyet et al., 1998a; Lefèvre et al., 1998), because of zonal spreading of the oversaturated equatorial water (equatorial upwelling of CO_2-rich deep waters). Nevertheless, sink regions for atmospheric CO_2 may appear in the equatorial latitude band because precipitation and river run-off can affect the fugacity (or partial pressure) of surface water CO_2, fCO_2. The largest rivers in the world discharge into the Atlantic ocean (Perry et al., 1996): the Amazon River in the west (0°, 50°W) and the

* Corresponding author. Centre IRD (Ex ORSTOM), B.P. 70, 29280-Plouzané, France. Tel.: +33-2-98-22-45-01; Fax: +33-2-98-22-45-14; E-mail: oudot@ird.fr

0304-4203/00/$ - see front matter
PII: S0304-4203(99)00077-8

Congo River in the east (6°S, 12°E). Previous papers showed how surface fCO_2 can be significantly affected by river run-off (Kempe and Pegler, 1991; Chen, 1993; Bakker et al., 1996; Frankignoulle et al., 1996; Kumar et al., 1996). Freshwater input by rivers decreases the ocean surface salinity and reduces concentration of total inorganic CO_2 and CO_2 fugacity. Considering the large discharge of the Amazon River ($1.93(\pm 0.01) \times 10^5$ m^3 s^{-1}, as reported by Perry et al., 1996) and the retroflection of the North Brazil Current (NBC) (Richardson and Reverdin, 1987), the resulting plume of low-salinity water influences a large portion of the western tropical Atlantic (Neumann, 1969; Muller-Karger et al., 1988; Dessier and Donguy, 1994). Using Coastal Zone Coastal Scanner (CZCS) climatologies, Lefèvre et al. (1998) discuss the eastward advection of the Amazon outflow by the North Equatorial Counter Current (NECC) as far as 25°W. Here, we present a data set that illustrates the effect of the Amazon run-off on the surface water fCO_2 in the western tropical Atlantic. Then, we discuss the physical and biological processes controlling the spatial variations of fCO_2 in that area, and finally, we estimate seasonal changes of the air–sea CO_2 flux deduced from the seasonal cycle of the sea surface salinity (SSS) in the region.

2. Data set

The data used in this study were obtained during the two ETAMBOT cruises carried out in boreal summer (9 September 1995–11 October 1995) and boreal spring (12 April 1996–16 May 1996), respectively, in the western tropical Atlantic (Fig. 1a) and the SABORD survey (25–29 May 1996) of the continental shelf off French Guiana (Fig. 1b). The ETAMBOT cruises were part of the French contribution to the WOCE Hydrographic Programme in the Atlantic ocean. Data were collected during the WOCE CITHER 1 cruise (January–March 1993) in the same region, but the results are not used in this study because of possible bias in the CITHER 1 fCO_2 data set.

The hydrographic and CO_2 data were collected in a similar fashion as during the CITHER 1 cruise carried out in the equatorial Atlantic ocean (Oudot et al., 1995). Sea surface water was sampled with a General Oceanics rosette system fitted to a Neil Brown CTDO probe (Gouriou, 1997a,b).

The measurement of fCO_2 in seawater was carried out by equilibrating an air stream with a thermostated (28.0°C) seawater sample (550 cm^3) in the sampling flask itself. The equilibrated air was injected into the IR analyzer (LICOR, model LI 6262) after passing through a desiccant (P_4O_{10}) column. The measured signal was compared with those produced by three standard gases (329.0–349.6–407.7 ppm), certified to ± 0.25 ppm by the French supplier (Air Liquide) and in agreement with the Scripps Institution of Oceanography (SIO) standard scale. The CO_2 fugacity was then calculated following Weiss (1974) taking the vapor pressure of water into account (Weiss and Price, 1980) and corrected for in situ temperature according to the temperature dependence equation described by Copin-Montegut (1989). The reproducibility of measurements, tested as the mean difference for duplicates, is 2.9 μatm during ETAMBOT 1 and 2.2 μatm during ETAMBOT 2 and SABORD. Due to calibration anomalies at the beginning of the ETAMBOT 1 cruise, calculated fCO_2 values (from TCO_2 and pH) are reported rather than measured fCO_2 data for the eight first stations of that cruise.

Atmospheric CO_2 concentration (ppm) was measured twice a day by continuously pumping for about 30 min an air stream, taken at a mast at the vessel's bow (about 10 m above the sea surface). The dried air stream was introduced into the IR analyzer and calibrated with the same standard gases as described previously. The CO_2 fugacity in the atmosphere (μatm) was then computed taking the water vapor pressure and the barometric pressure into account. The uncertainty for the atmospheric CO_2 concentration is estimated at ± 0.3 ppm (± 0.3 μatm for the atmospheric CO_2 fugacity).

Measurements of total inorganic carbon, TCO_2, were made by gas chromatography (Oudot et al., 1995) and their reproducibility, determined as the mean difference of duplicates (two bottles fired at the same depth), is 7 μmol kg^{-1} during ETAMBOT 1 and 10 μmol kg^{-1} during ETAMBOT 2 and SABORD. The accuracy was checked against Certified Reference Material provided by A.G. Dickson (Scripps Institution of Oceanography).

The total alkalinity of seawater, TA, was determined from TCO_2 and pH measurements using the UNESCO (1987) definition:

$$TA = [HCO_3^-] + 2[CO_3^{2-}] + [B(OH)_4^-] + [OH^-] - [H^+]. \quad (1)$$

$[HCO_3^-]$ and $[CO_3^{2-}]$ were deduced from TCO_2 measurements and pH measurements. The pH measurements were based on the total hydrogen ion concentration scale (Dickson, 1993), and the Ross combination electrode (ORION, model 81-02) was calibrated in 0.04 M Tris and 0.04 M AMP buffers prepared according to Dickson (1993). The reproducibility of pH measurements, tested as the mean difference of duplicates is 0.002 and 0.003 during ETAMBOT 1 and ETAMBOT 2, respectively. The equations used for determination of the dissociation constants relative to the 'total' pH scale were those of Roy et al. (1993) for carbonic acid, Dickson (1990) for boric acid and Millero (1995) for ionization of water. The reproducibility of TA results, tested as the mean difference of duplicates, is similar to that of TCO_2 measurements: 7 μmol kg^{-1} during ETAMBOT 1 and 10 μmol kg^{-1} during ETAMBOT 2 and SABORD.

The nutrient (silicate) concentrations were measured according to the standard method (Mullin and Riley, 1955) in a BRAN + LUEBBE Auto-Analyzer equipped with an automated data acquisition system. The analytical precision (±1 SD) was 0.2 μmol kg^{-1} for silicate (Baurand and Oudot, 1997a,b) for each cruise.

3. Results: fCO_2 distributions

fCO_2 data obtained along the cruise track during ETAMBOT 1 and ETAMBOT 2 are shown in Fig. 2, together temperature and salinity. The mean value of atmospheric CO_2 fugacity during both cruises is depicted as straight lines for ETAMBOT 1 (347.0 μatm — full line) and ETAMBOT 2 (352.5 μatm — dashed line) to illustrate the CO_2 sink (oceanic fCO_2 < atmospheric fCO_2) and source (oceanic fCO_2 > atmospheric fCO_2) areas. Near the coast, at the beginning of ETAMBOT 1 and the end of ETAMBOT 2, the oceanic fCO_2 decreases down to 200 μatm (i.e., 150 μatm below the atmospheric level), while, in the open ocean the highest fCO_2 level remains below 400 μatm (i.e., only 50 μatm above the atmospheric level). Results collected during the SABORD survey are shown in the same way in Fig. 3: the continental shelf is a strong CO_2 sink everywhere with the ocean–atmosphere fCO_2 difference reaching more than 200 μatm.

In both figures, spatial variations of oceanic fCO_2 are closely related to those of salinity. During ETAMBOT 1, which was carried out during late summer–early fall, the salinity field is strongly influenced by the Amazon Plume water transported offshore in the NBC retroflection (Lentz, 1995). The low-salinity (< 33.0) and low-fugacity (~ 320 μatm) water extends eastwards to about 35°W, over 2000 km from the river mouth (Fig. 2). The eastward extension of the low-salinity plume is not continuous due to the influence of the NBC retroflection eddies and the meandering of the NECC (Richardson et al., 1994; Bourlès et al., 1999). During ETAMBOT 2 that started in April, a few weeks before the maximum Amazon discharge (Lentz, 1995), the SSS (~ 36.0) as well as fCO_2 (on the average ~ 360 μatm) are generally high, except in front of the Amazon mouth (start of leg D, Fig. 2b) and in front of Cayenne at the end of the cruise, in mid-May (leg E, Fig. 2b).

On the French Guiana continental shelf (SABORD), both the salinity and fCO_2 values increase from inshore to offshore along each leg at the end of May (Fig. 3). There is also an increasing trend of salinity and fCO_2 northwestwards along the coast, i.e., downstream the plume carried by the northwestward boundary current. The very fresh waters encountered during the cruise, as well as those identified two weeks earlier (ETAMBOT 2 — leg E) in front of Cayenne, probably correspond to relatively pure Amazon water that also exhibits the most pronounced fCO_2 signature. High silicate concentrations (up to 45 μmol kg^{-1}) measured on the continental shelf confirm the riverine origin of these waters.

No clear temperature–fCO_2 relationship is evidenced in the oceanic CO_2 fugacity distributions. This absence of relationship was previously shown (Oudot et al., 1987) in tropical Atlantic, except north of 5°N in boreal winter where surface-layer cooling

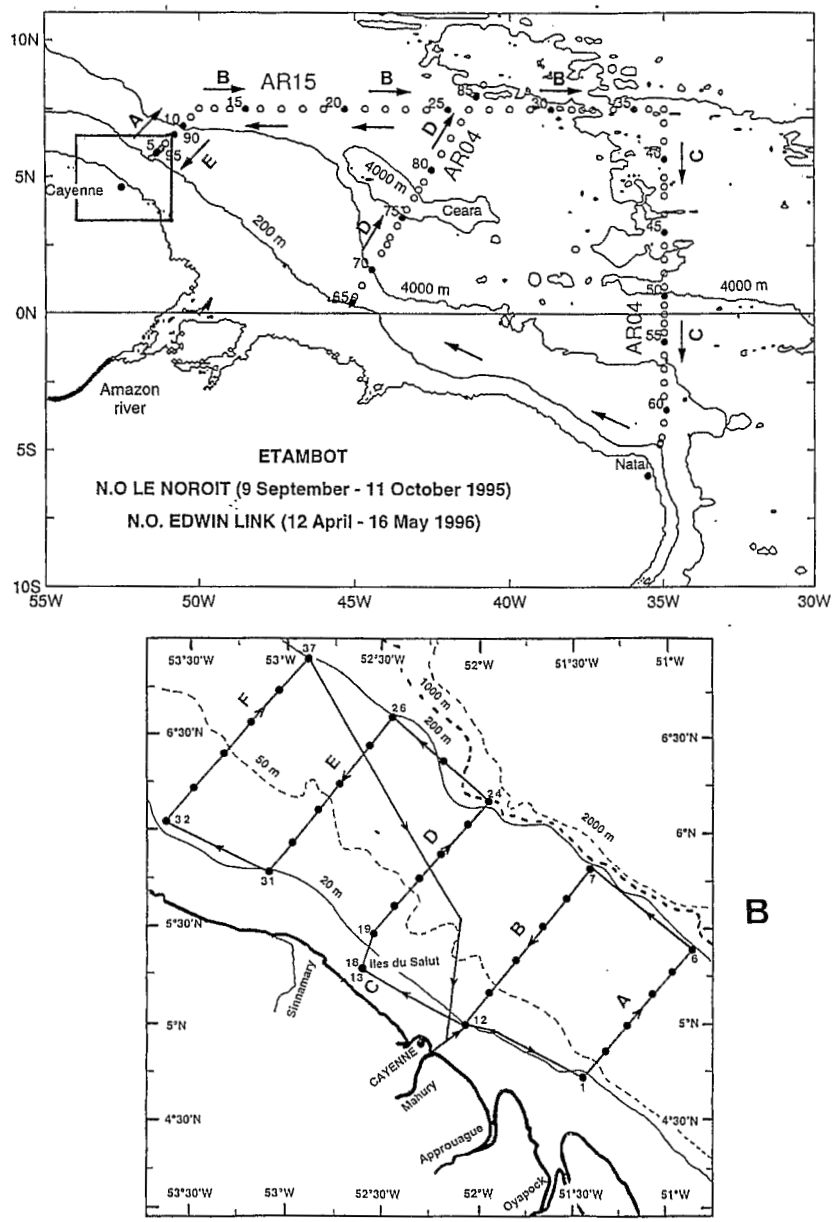

Fig. 1. Cruise tracks and stations location during (A) ETAMBOT 1 (9 September 1995–11 October 1995) and ETAMBOT 2 (12 April 1996–16 May 1996), and (B) SABORD (25–29 May 1996). The square in (A) indicates the position of (B).

may lower the oceanic fCO_2 value. However, during ETAMBOT 2 which is made just in early spring, the slight decrease of oceanic fCO_2 below the atmospheric level, at the end of leg B (Fig. 2c), may be related to the observed temperature decrease (Fig. 2a). Thus, oceanic fCO_2 corrected at a constant temperature (28°C), according to the CO_2-solubility temperature dependence of 4.23% $°C^{-1}$ for constant total CO_2 (Takahashi et al., 1993), varies much less and remains above the atmospheric level during

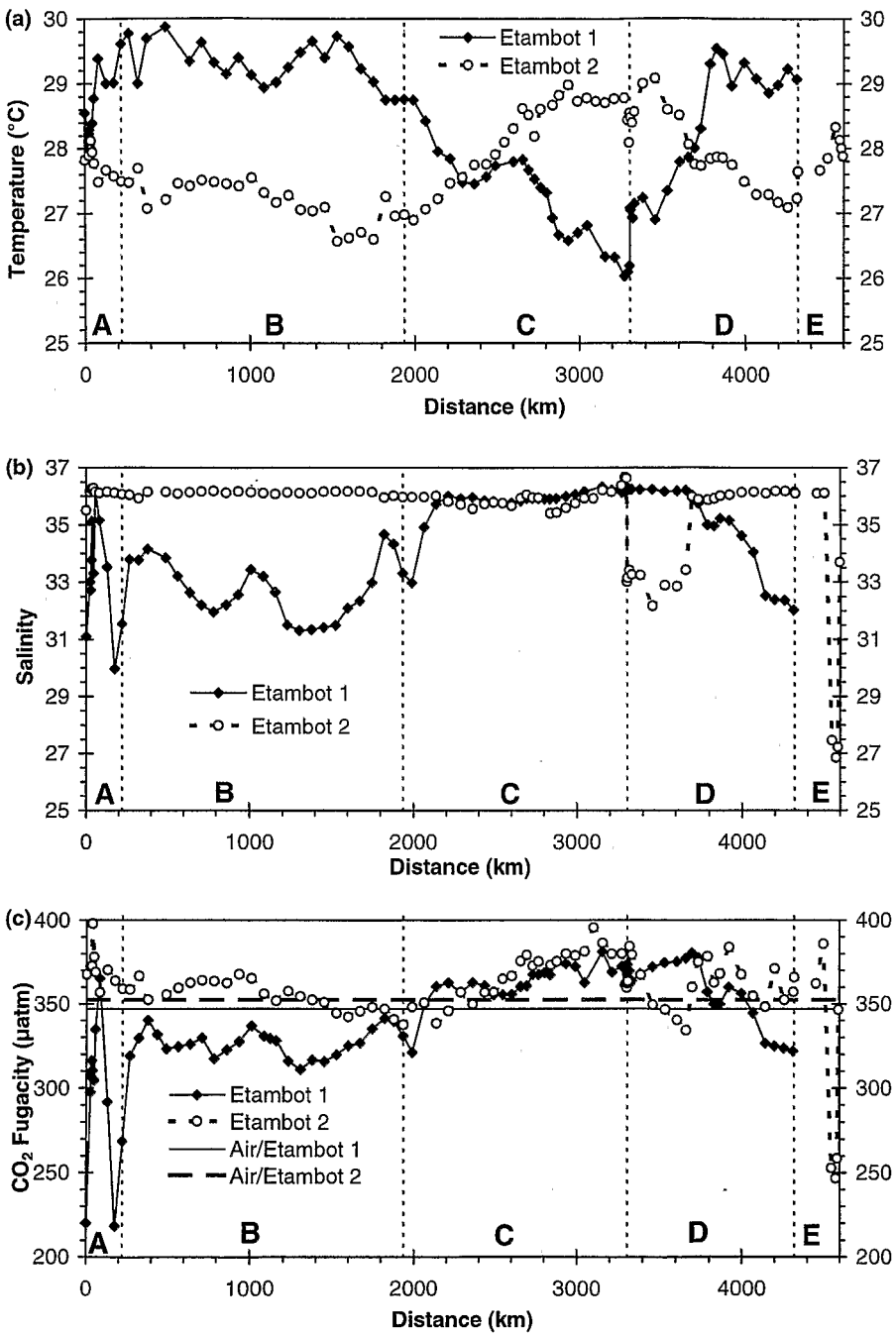

Fig. 2. Variations of (a) temperature (°C), (b) salinity and (c) fugacity of CO_2 (µatm) at the sea surface along the cruise tracks of ETAMBOT 1 and ETAMBOT 2. Mean values of atmospheric CO_2 fugacity are indicated by straight lines (347.0 µatm for ETAMBOT 1 and 352.5 µatm for ETAMBOT 2). Letters correspond to the different legs of the cruises (Fig. 1a). The CO_2 fugacity data of ETAMBOT 1 on legs A and B for the first 600 km of the ship's route are calculated from TCO_2 and pH, and are omitted in Fig. 5a.

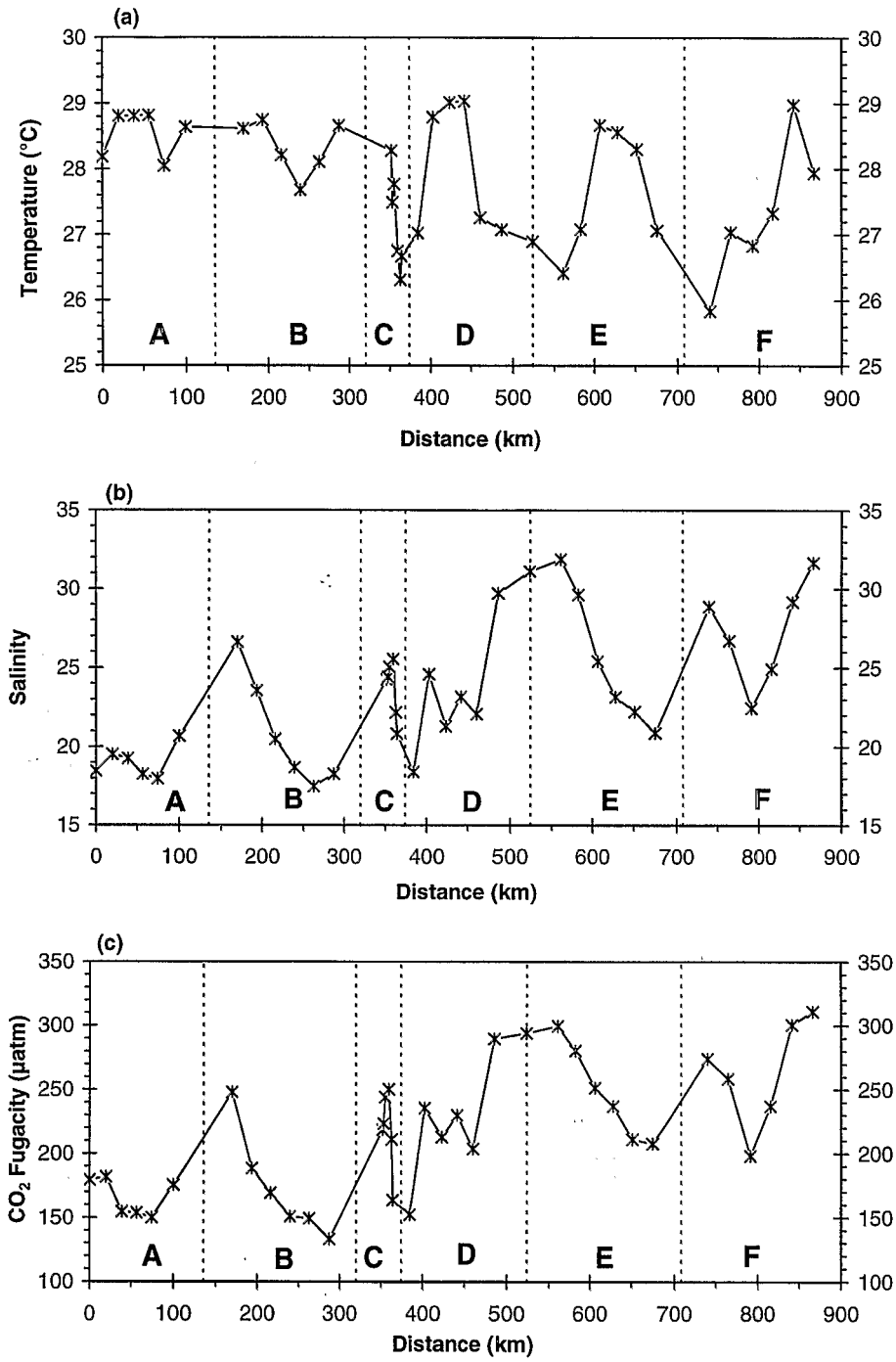

Fig. 3. Variations of (a) temperature (°C), (b) salinity and (c) fugacity of CO_2 (µatm) at the sea surface along the SABORD cruise track. Letters correspond to the different legs of the survey (Fig. 1). Mean value of atmospheric CO_2 fugacity (not shown) is 352.5 µatm as determined during ETAMBOT 2.

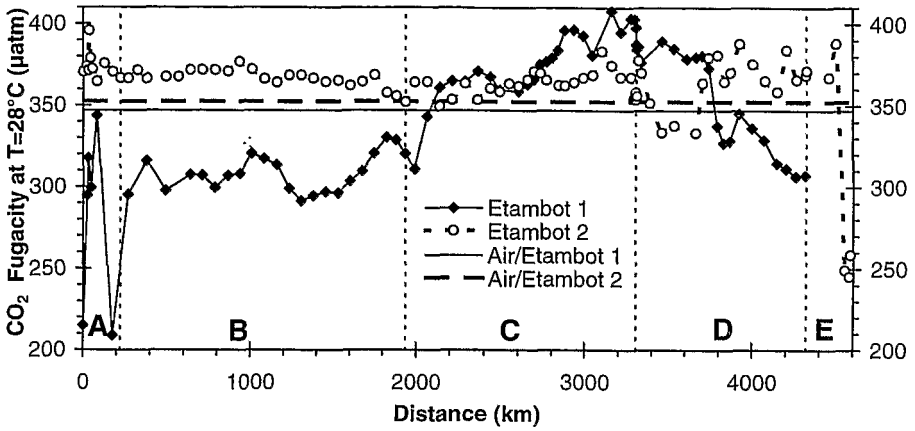

Fig. 4. Variations of fugacity of CO_2 (µatm) measured at $T = 28°C$ at the sea surface along the cruise tracks of ETAMBOT 1 and ETAMBOT 2. Mean values of atmospheric CO_2 fugacity are indicated by straight lines (347.0 µatm for ETAMBOT 1 and 352.5 µatm for ETAMBOT 2). Letters correspond to the different legs of the cruises (Fig. 1a).

ETAMBOT 2 (Fig. 4), except where salinity strongly decreases.

4. Discussion: physical and biological processes for CO_2 sink

As expected from the similar distribution patterns of fCO_2 and salinity in surface waters (Figs. 2 and 3), we found a high correlation ($r = 0.979$) between CO_2 fugacity and salinity at the sea surface in the western equatorial region (Fig. 5a), irrespective of the season. That relationship between fCO_2 and salinity suggests that the decrease in oceanic fCO_2 below the atmospheric level is closely related to Amazon discharge and the subsequent spreading of freshwater by the surface oceanic circulation. Such a salinity decrease in the area cannot be the result of precipitation: the rainfall map of Dorman and Bourke (1981), as well as the freshwater budget of Yoo and Carton (1990) in the tropical Atlantic ocean, suggest that the influence of precipitation is negligible in comparison to the Amazon River discharge. On the other hand, the strong inverse correlation between salinity and silicate (Fig. 5b) strongly suggests that the decrease in salinity is related to the river discharge (Froelich et al., 1978; Key et al., 1985).

However, processes other than physical ones (mixing between ocean water and river freshwater, precipitation, temperature decrease) contribute to lower fCO_2. Biological activity also may decrease the oceanic CO_2 fugacity by photosynthetic CO_2 uptake. It is possible to estimate the dilution effect of freshwater on the fCO_2 distribution by computing fCO_2 expected from the mixing between ocean water and river water. Expected fCO_2 is calculated (dotted line in Fig. 5a), at a given salinity and the mean sea surface temperature (SST) in the region (28°C), from TCO_2 and TA values resulting from the conservative mixing between the two endmembers. According to the ETAMBOT data set (Fig. 5c–d), the seawater component values are:

$$\text{Ocean water:}\quad S = 36.2 \quad TCO_2 = 2018\ \mu\text{mol kg}^{-1}$$
$$TA = 2403\ \mu\text{mol kg}^{-1} \qquad (2)$$

To estimate the Amazon River endmember, we refer to Richey et al. (1990) which indicate a TCO_2 concentration of 500–600 µmol kg^{-1} downstream (in a more recent study, Richey et al., 1991 mention a range of 485–667 µmol kg^{-1} at the most downriver site); the TCO_2 values were slightly greater during rising water (March) than falling water (September). We neglect the decomposition of organic carbon of which the concentration is comparable to inorganic carbon, because a large proportion of the organic matter is refractory (Richey et al., 1990). As the hydrogen carbonate is the predominant form of

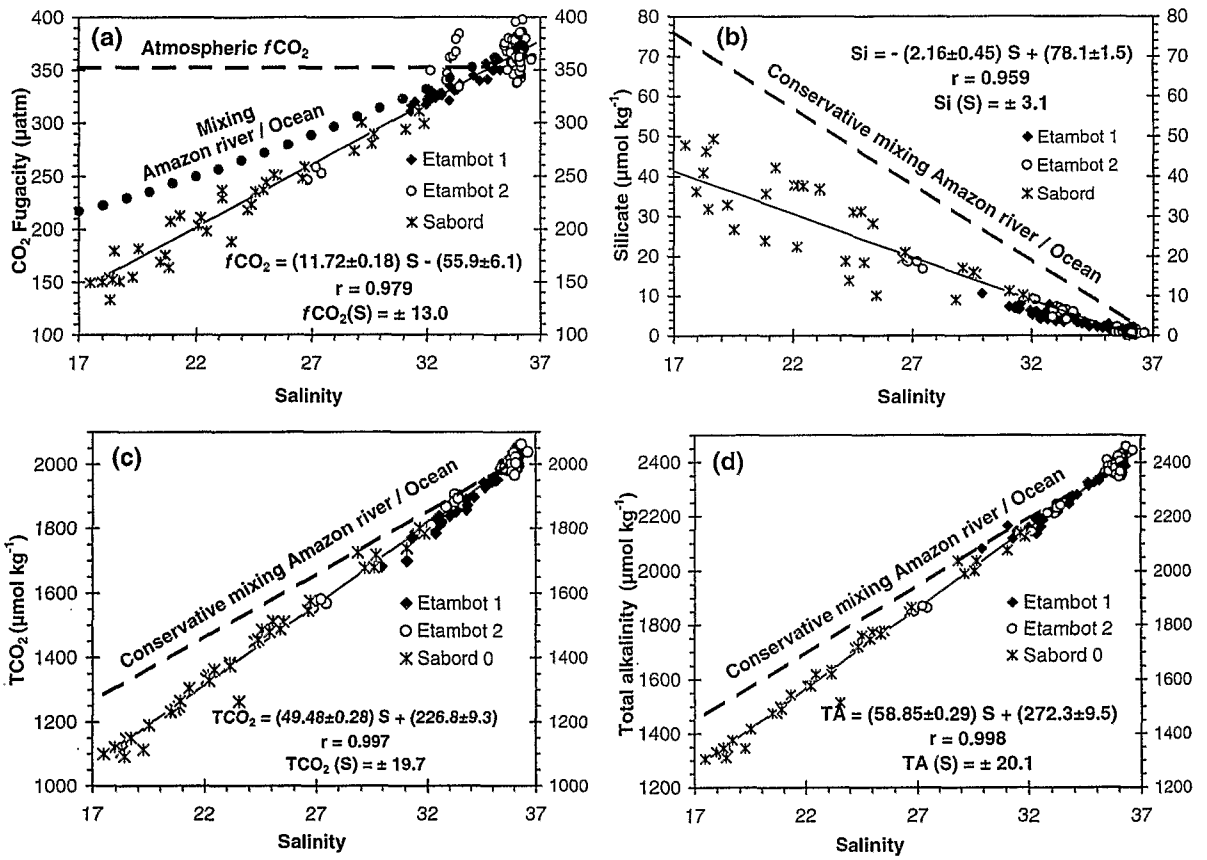

Fig. 5. (a) Relationship between CO_2 fugacity (µatm) and salinity at the sea surface during ETAMBOT 1, ETAMBOT 2 and SABORD. The equation and correlation coefficient, r, are for the regression line (solid line) fitted to the data. fCO_2 (S) indicates the uncertainty in fCO_2 calculated from salinity–fCO_2 regression equation. The dotted line represents expected fCO_2 from the mixing between ocean water and river water: expected fCO_2 is calculated at a given salinity and the mean sea surface temperature in the region (28°C) from TCO_2 and TA values resulting from the conservative mixing between river and sea waters, whose endmembers are defined in the text. (b) Relationship between silicate (µmol kg^{-1}) and salinity at the sea surface during ETAMBOT 1, ETAMBOT 2 and SABORD. The equation and correlation coefficient, r, are for the regression line (solid line) fitted to the data. Si (S) indicates the uncertainty in silicate calculated from salinity–silicate regression equation. The dashed line represents the conservative mixing between river and sea waters, whose endmembers are defined in the text. (c) Relationship between total inorganic carbon TCO_2 (µmol kg^{-1}) and salinity at the sea surface during ETAMBOT 1, ETAMBOT 2 and SABORD. The equation and correlation coefficient, r, are for the regression line (solid line) fitted to the data. TCO_2 (S) indicates the uncertainty in TCO_2 calculated from salinity–TCO_2 regression equation. The dashed line represents the conservative mixing between river and sea waters, whose endmembers are defined in the text. (d) Relationship between total alkalinity TA (µmol kg^{-1}) and salinity at the sea surface during ETAMBOT 1, ETAMBOT 2 and SABORD. The equation and correlation coefficient, r, are for the regression line (solid line) fitted to the data. TA (S) indicates the uncertainty in TA calculated from salinity–TA regression equation. The dashed line represents the conservative mixing between river and sea waters, whose endmembers are defined in the text.

the inorganic carbon in the Amazon water (Richey et al., 1990), the river endmember value of TA may be considered to be equal to the TCO_2 value, as mentioned by Olsson and Anderson (1997). The choice of the TCO_2 and TA values in Amazon River water will govern the depression of fCO_2 by mixing. As the Sabord survey occurred in May, we adopt the TCO_2 and TA values observed during rising water and the river water endmembers are:

$$\text{River water:}\quad S=0\quad TCO_2=600\ \mu\text{mol kg}^{-1}$$
$$TA=600\ \mu\text{mol kg}^{-1}. \qquad (3)$$

For a salinity of 17.5, TCO_2 and TA expected from the conservative mixing are 1285 and 1472 μmol kg^{-1}, respectively, and the corresponding calculated fCO_2 value is 219 μatm. As the mean observed CO_2 fugacity of the ocean water ($S = 36.2$) is about 368 μatm (Fig. 5a), the maximal depression in fCO_2 expected from the mixing effect is 149 μatm, i.e., about 67% of the maximal observed fCO_2 decrease (220 μatm). The biological processes should therefore account for nearly third of the observed depression in oceanic fCO_2. If we used lower TCO_2 and TA values of 500 μmol kg^{-1} in river water, the expected fCO_2 will be lowered by 16 μatm and the biological depression would be yet a quarter of the observed depression in oceanic fCO_2, that does not alter our conclusions.

Some of the ETAMBOT 2 data, with salinity around 33, are closer to the mixing line than to the regression line (Fig. 5a). They correspond to samples, collected in front of the Amazon estuary, for which the biological uptake of CO_2 should be reduced, probably because of less favorable conditions of biological production (greater turbidity).

The biological activity effect (photosynthesis/respiration or carbonate production/dissolution) is also visible on the plots of total inorganic carbon TCO_2 and total alkalinity TA vs. salinity (Fig. 5c–d), and silicate vs. salinity (Fig. 5b). As for fCO_2 data, the TCO_2, TA and silicate fall below the conservative mixing lines. The mixing lines for TCO_2 and TA (Fig. 5c–d) are drawn from the endmember values previously defined in (2) and (3). The mixing line for silicate (Fig. 5b) is constructed from Amazon River estuary surface samples (Table 2 in Key et al., 1985) and from mean oceanic concentration determined during our cruises, resulting in the following endmembers:

$$\text{Ocean water:} \quad S = 36.2 \quad \text{Silicate} = 2\ \mu\text{mol}\,\text{kg}^{-1} \tag{4}$$

$$\text{River water:} \quad S = 0 \quad \text{Silicate} = 142\ \mu\text{mol}\,\text{kg}^{-1}. \tag{5}$$

DeMaster and Pope (1996) found 144 μmol kg^{-1} as silicate concentration in the riverine endmember, based on AMASSEDS results.

The silica data, as well as those of TCO_2 and TA, illustrate the biological removal of carbon and silica in sea surface water by calcifying and siliceous organisms. From the maximum TCO_2 deficit recorded in the SABORD data, which is about 200 μmol kg^{-1} (Fig. 5c), we can estimate the primary production rate. Lentz and Limeburner (1995) give an averaged low-salinity layer thickness of 5 ± 2 m within the Amazon Plume, which rarely exceeds 10 m. The thickness of the low-salinity layer on the continental shelf, in front of French Guiana, ranges from 10 to 15 m during SABORD, while the depth of the surface mixed layer is 15 to 20 m, based on a study of the barrier layer in the western equatorial Atlantic (Pailler et al., 1999). From these considerations, we therefore assume that the CO_2 biological consumption occurs in a 10 ± 5 m thick layer. Lentz and Limeburner (1995) estimated the mass and salinity budget of the plume northwestward from the Amazon mouth, based on an along-plume velocity of 40 cm s^{-1}. From this crude estimate, we predict that biological uptake of CO_2 occurred during the water mass transit of 20 days from the river mouth to the French Guiana shelf, which is probably an upper limit as deduced from a tracer budget. With such a residence time, the rate of productivity rate is:

$$\begin{aligned}&[200 * (10 \pm 5)]/[20]\\ &\quad = 100.0 \pm 72.5\ \text{mmol}\,\text{C}\,\text{m}^{-2}\,\text{day}^{-1}\\ &\quad = 1.2 \pm 0.9\ \text{g}\,\text{C}\,\text{m}^{-2}\,\text{day}^{-1}.\end{aligned} \tag{6}$$

On the other hand, direct current measurements (satellite drifter observations according to Limeburner et al., 1995, moored array according to Lentz and Limeburner, 1995 and Acoustic Doppler Current Profiler according to Bourlès, personal communication) described the near-surface velocity fields over the North Brazil and Guiana shelves, respectively. These measurements lead us to estimate a lower transit time along the continental shelf of about 15 days, using a mean velocity of 50 cm s^{-1} between the river mouth and 6°N. With this transit time, the productivity rate amounts to:

$$\begin{aligned}&[200 * (10 \pm 5)]/[15]\\ &\quad = 133.3 \pm 96.7\ \text{mmol}\,\text{C}\,\text{m}^{-2}\,\text{day}^{-1}\\ &\quad = 1.6 \pm 1.2\ \text{g}\,\text{C}\,\text{m}^{-2}\,\text{day}^{-1}.\end{aligned} \tag{7}$$

These estimates have to be corrected for the air–sea flux of CO_2 as, the continental shelf area

being a strong CO_2 sink, the resulting entering flux of atmospheric CO_2 into the sea underestimates the depression of fCO_2 due to the biological productivity. The net air–sea flux is estimated to be -15 mmol m^{-2} day^{-1} (i.e., -0.18 g C m^{-2} day^{-1}) or -24 mmol m^{-2} day^{-1} (i.e., -0.29 g C m^{-2} day^{-1}) as described below (the two results corresponding to two different calculation models). This correction (0.2 to 0.3 g C m^{-2} day^{-1}) is negligible in comparison with the uncertainty of our estimation of the productivity rate expected from the CO_2 deficit.

The rough estimate of the primary production, which is responsible of third of the fCO_2 depression, is compared with the assessment of the primary productivity from ^{14}C-uptake experiments on the continental shelf within the plume of the Amazon River, during AMASSEDS (Smith and DeMaster, 1996). The mean productivity ranges from 2.2 in turbid nutrient rich water to 0.8 g C m^{-2} day^{-1} in clear offshore regions. Cadee (1975) estimated a mean primary production rate of 0.9 g C m^{-2} day^{-1} in the 20–60 m depth region of the French Guiana continental shelf, which was five times that measured offshore. Our results (1.6 ± 1.2 and 1.2 ± 0.9 g C m^{-2} day^{-1}) are in reasonable agreement with the upper and lower limits of direct measurements of primary productivity in the Amazon estuary and in the zone directly influenced by the Amazon river plume, given the crudeness of the estimates. Thus, the biological activity in the surface water affected by the Amazon discharge contributes significantly to the CO_2 sink that seasonally appears in the western equatorial Atlantic ocean.

From comparison between the regression line fitted to data and the conservative mixing line, the maximum depression in silicate (Fig. 5b) due to biological activity is approximately 35 μmol kg^{-1}, which is in agreement with the highest silicate depletion (over 30 μmol kg^{-1}) reported by DeMaster and Pope (1996) on the Amazon shelf. To compare silicate and inorganic carbon depletion involved in biological uptake (maximum depression of 35 and 200 μmol kg^{-1}, respectively), we have to correct the inorganic carbon depletion for calcification. The observed TA deviation away from the conservative line (172 μmol kg^{-1} for $S = 17.5$, Fig. 5d) is characteristic of calcium carbonate production in seawater (Broecker and Peng, 1982). As the change in TA due to carbonate mineral production is twice as large as the change in TCO_2 (Skirrow, 1975) and by neglecting the small changes of TA due to production and decay of organic matter (Brewer and Goldman, 1976), the organic carbon production corrected for calcification is $200 - 172/2 = 114$ μmol kg^{-1}. Thus, silicate and inorganic uptake are in a molar ratio $Si/C = 0.31$, in the range (0.15–0.4) of the molar silicon/carbon production ratio reported by DeMaster et al. (1996) in the waters of the Amazon shelf. This relatively high value (0.31) in comparison to the mean of 0.13 for low-latitude diatoms (Brzezinski, 1985) underlines the dominant role of diatoms in the primary production in this zone.

5. Air–sea fluxes of CO_2

5.1. Flux calculation procedure

Air–sea fluxes are estimated from the observed fCO_2 data and the relationship:

$$F = k_t \alpha \Delta fCO_2 \quad (8)$$

where k_t is the CO_2 gas transfer velocity, α is CO_2 solubility in seawater (Weiss, 1974) and ΔfCO_2 is the difference between the CO_2 fugacity in the ocean and that in the atmosphere ($\Delta fCO_2 = fCO_2^{sea} - fCO_2^{air}$). The CO_2 flux is positive when CO_2 escapes from the ocean into the atmosphere and negative otherwise. While α and ΔfCO_2 are easily calculated, k_t is difficult to estimate because of its dependence on several factors (wind speed, sea surface roughness, bubbles, thermal skin effect). Different ways have been shown to compute this coefficient from wind speed, and take these effects into account (Broecker and Siems, 1984; Liss and Merlivat, 1986; Tans et al., 1990; Watson et al., 1991; Robertson and Watson, 1992; Wanninkhof, 1992; Van Scoy et al., 1995; McNeil and Merlivat, 1996). We chose to compute the air–sea CO_2 fluxes with two relationships: that of Liss and Merlivat (1986) (thereafter L&M86), we used in our previous studies (Andrié et al., 1986; Oudot et al., 1995) but often suspected to yield low fluxes, and the more recent relationship of Wanninkhof (1992) (thereafter Wkf92), that yields higher fluxes (Bakker et al., 1997) and whose gas flux parameterization for climatological winds is in

best agreement with observations (Haines et al., 1997). Considering the uncertainty in the relationships between wind speed and air–sea gas exchange, we ignored the thermal skin effect on the air–sea CO_2 flux (Van Scoy et al., 1995).

Liss and Merlivat (1986) equations for different wind regimes are:

$$k_{20} = 0.17V \quad \text{for } 0 < V < 3.6\,\text{m s}^{-1} \tag{9}$$

$$k_{20} = 2.85V - 9.65 \quad \text{for } 3.6 < V < 13.0\,\text{m s}^{-1} \tag{10}$$

where k_{20} is the transfer velocity (or exchange coefficient) for CO_2 at 20°C expressed in cm h^{-1} and V is the wind speed at 10 m above the sea level, expressed in m s^{-1}. The wind data we used to compute the transfer velocity are extracted from an atlas of the tropical Atlantic wind stress climatology (2° × 2° gridded monthly mean, Servain et al., 1987) constructed from measurements made aboard volunteer observing ships (Bourlès and Marin, 1997; Marin, 1997). For the whole continental shelf, we adopted the average wind speed measured at sea during the cruise, which is very similar to the climatological wind. The exchange coefficient depends on the temperature:

$$k_t = k_{20}(Sc_t/600)^{-2/3} \quad \text{for } 0 < V < 3.6\,\text{m s}^{-1} \tag{11}$$

$$k_t = k_{20}(Sc_t/600)^{-1/2} \quad \text{for } 3.6 < V < 13.0\,\text{m s}^{-1} \tag{12}$$

where Sc_t, the Schmidt number for CO_2 at t°C, is determined using the polynomial relationship of Wkf92:

$$Sc_t = 2073.1 - 125.62t + 3.6276t^2 - 0.043219t^3. \tag{13}$$

Wkf92 proposed two relationships to calculate the gas transfer velocity: one for short-term wind speed data (shipboard measurements, scatterometer and radiometer data) and another one for long-term averaged wind speed data (related to ^{14}C invasion):

$$k_{st} = 0.31V_{st}^2(660/Sc_t)^{1/2} \quad \text{for short-term wind} \tag{14}$$

$$k_{lt} = 0.39V_{lt}^2(660/Sc_t)^{1/2} \quad \text{for long-term wind} \tag{15}$$

where k_{st} and k_{lt} are expressed in cm h^{-1} and V_{st} and V_{lt} are expressed in m s^{-1}. The Schmidt number of CO_2 in seawater at temperature = 20°C is 660 (Wanninkhof, 1992).

5.2. Flux results

Fig. 6 shows the distribution of CO_2 fluxes calculated according to the Wkf92 parameterization for short-term wind (Eq. (14)), from fCO_2 data and wind speed along both ETAMBOT cruises tracks and along the SABORD one. The net CO_2 fluxes along each leg of the ETAMBOT cruises and on the French Guiana continental shelf, calculated according to the two parameterizations (L&M86 and Wkf92), are compared in Table 1. These results show the lower CO_2 fluxes calculated according to the L&M86 parameterization in comparison with the Wkf92 CO_2 fluxes (Bakker et al., 1997; Goyet et al., 1998b). On average, the L&M86 fluxes differ from the Wkf92 ones by 80%, but differences may be beyond 130% (Table 1). At 7.5°N (Leg A + Leg B), the mean CO_2 flux is entering into the sea during ETAMBOT 1 and escaping during ETAMBOT 2, except at the end of that latter cruise (Leg E) when it becomes a strong invasion, because of the fCO_2 decrease associated to the freshwater pool. Along the 35°W and Ceara sections (Leg C and Leg D, Fig. 1, top panel), CO_2 escapes from the ocean during both ETAMBOT cruises (Table 1). The amplitude of CO_2 flux variations is higher during ETAMBOT 2 than during ETAMBOT 1 (Fig. 6) as the wind speed north of the equator is higher in boreal spring (ETAMBOT 2) than in late summer–fall (ETAMBOT 1), as a result of the north–south migration of the Intertropical Convergence Zone during the year. The CO_2 sink observed in boreal spring 2000 km away from the coast, in open ocean (35–40°W) at 7.5°N (Fig. 6, ETAMBOT 2) is caused by winter cooling of the sea surface (Oudot et al., 1987). The CO_2 sink observed during ETAMBOT 1 along the 7.5°N section (Leg B) is smaller than the previously described one (ETAMBOT 2) due to lower wind speed in late summer–fall and is related to the eastward spreading of low-salinity water (Fig. 2b). The strong CO_2 sink observed at the end of ETAMBOT 2, which was not present 1 month earlier (Fig. 6, ETAMBOT 2) or a few days later on the continen-

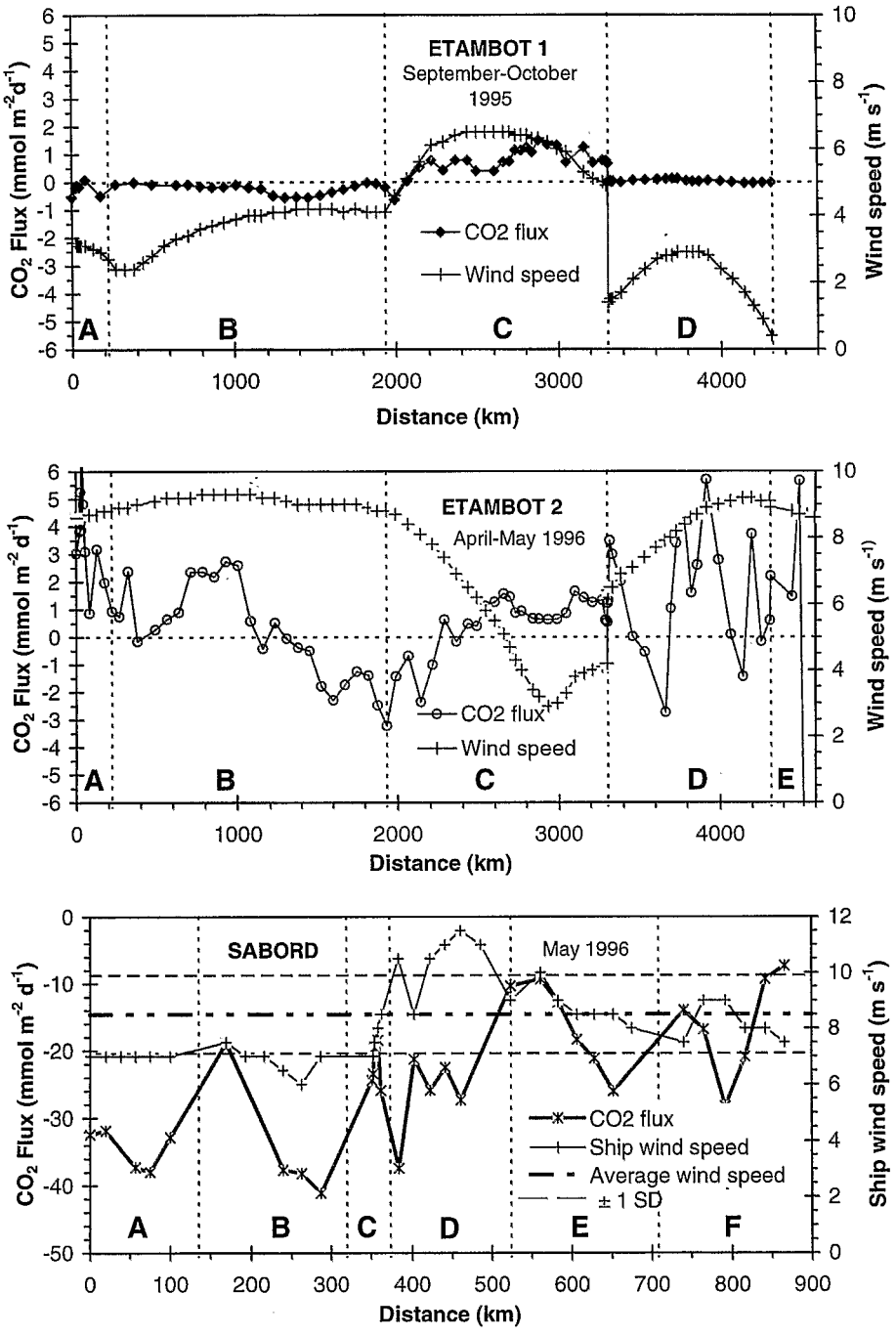

Fig. 6. Variations of CO_2 flux (mmol m^{-2} day^{-1}) at the air–sea interface and wind speed (m s^{-1}) along cruise tracks of ETAMBOT 1 and ETAMBOT 2, and SABORD. The CO_2 flux is computed according to the parameterization of Wkf92. The CO_2 flux is positive when CO_2 escapes from the sea into the atmosphere and negative otherwise. Letters correspond to the different legs of the cruises (Fig. 1).

Table 1
CO_2 flux (mmol m^{-2} day^{-1}) computed according to the parameterizations of L&M86 and Wkf92 along each leg of ETAMBOT cruises and SABORD survey. Δ % represents the relative increase of CO_2 flux (Wkf92) vs. CO_2 flux (L&M86) (Δ % = 2(Wkf92 − L&M86)/(Wkf92 + L&M86))

	ETAMBOT 1 (September–October 1995)			ETAMBOT 2 (April – May 1996)		
	L&M86	Wkf92	Δ %	L&M86	Wkf92	Δ %
Cayenne — 50°W, 7.5°N (Leg A)	−0.21 ± 0.21	−1.17 ± 1.17	139	2.05 ± 1.28	3.32 ± 2.07	47
Section 7.5°N (50°W–35°W) (Leg B)	−0.22 ± 0.18	−0.69 ± 0.42	103	0.06 ± 1.03	0.11 ± 1.71	59
Section 35°W (7.5°N–5°S) (Leg C)	0.74 ± 0.48	1.16 ± 0.81	44	0.08 ± 0.66	0.40 ± 1.19	133
Section Ceara (0°, 45°W–8°N, 41°W) (Leg D)	0.04 ± 0.05	0.18 ± 0.22	127	0.95 ± 1.24	1.52 ± 1.99	46
50°W, 7.5°N — Cayenne (Leg E)				−11.53 ± 0.69	−18.68 ± 1.13	47

	SABORD (May 1996)		
Continental shelf in front of French Guiana	L&M86	Wkf92	Δ %
Mean (Legs A + B + C + D + E + F)	−15.0 ± 5.9	−24.2 ± 9.5	47

tal shelf, is also related to the arrival of a freshwater lens originating from the Amazon mouth region and propagating northwestward along the coastline. The net CO_2 flux on the continental shelf is an order of magnitude (−24 mmol m^{-2} day^{-1}, after Wkf92) greater than the net CO_2 flux offshore (open sea areas) (Table 1).

5.3. Variability of the net CO_2 flux

Considering the strong regional relationship between oceanic fCO_2 and salinity (Fig. 5a), we infer the variability of the air–sea CO_2 flux in the western part of the equatorial belt, under the influence of the Amazon River outflow, from the variability of the SSS. Dessier and Donguy (1994) analyzed the seasonal and interannual variations of the SSS in the tropical Atlantic (15°S–30°N, 80°W–15°W) from observations collected by merchant ships between 1977 and 1989 (see in Fig. 7 the AX11 and AX20 WOCE XBT lines which indicate the track of the volunteer observing ships). They identified a well-defined seasonal cycle of SSS, related to river outflow (Amazon and Orinoco, northward at 8.5°N, 60.5°W) regimes. Near shore (5°N) the mean SSS cycle shows a minimum in May occurring just after the maximum Amazon outflow (Fig. 8a). Northeast of the shiptrack between Europe and French Guiana, the salinity minimum occurred in September–October near 10°N. This corresponds to the eastward advection of the freshwater pool by the NECC. In the zonal belt 5°N–10°N (Fig. 8b), the low-salinity plume ($S < 35$) extends eastward as far as 35°W.

The air–sea flux of CO_2, averaged over the whole area 5°S–10°N, 65°W–35°W, is calculated by bulk

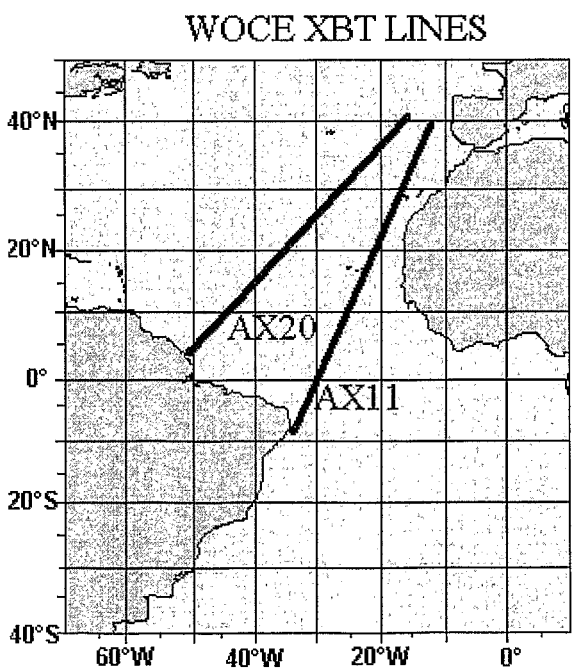

Fig. 7. Tracks of volunteer observing ships indicated by the WOCE XBT lines (AX20 between Europe and French Guiana and AX11 between Europe and Brazil).

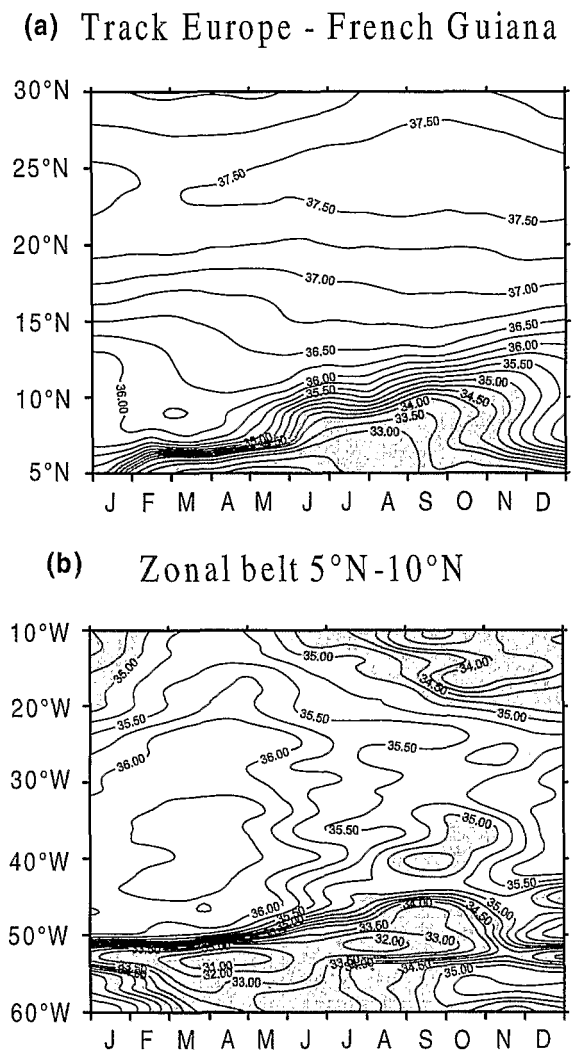

Fig. 8. Mean annual cycles of the sea surface salinity (space–time diagram) for the period 1977–1997, (a) along the shipping route from Europe to French Guiana and (b) in the zonal belt 5°N–10°N (from the South American coast to the African coast).

parameterization using climatologies of SST, wind velocity, salinity, and the fCO_2 gradient between atmosphere and ocean. Within these latitudinal boundaries (5°S–10°N), the reduced mean annual variability of SST (< 2°C) could induce a limited effect on fCO_2 variability (< 9%, according to the CO_2-solubility temperature dependence of 4.23% $°C^{-1}$ for constant total CO_2 of Takahashi et al., 1993) in comparison with fCO_2 variability induced by variability of salinity (~ 60%, if we refer to the range of variation of fCO_2 at 28°C, 210–400 μatm in Fig. 4). Monthly climatological fields of SST and wind velocity have been extracted from the COADS monthly climatology [1]. SSS has been documented by updated long-term (1977–1997) monthly mean charts on a 1° × 1° grid constructed by objective analysis of all available data (bucket samples collected by merchant ships of the IRD — Institut de Recherche pour le Développement, previously Institut Français de Recherche pour le Développement en Coopération, ORSTOM — network completed with NODC World Ocean Atlas surface data for area without observations) (see Dessier and Donguy, 1994 for the kriging method). The oceanic fCO_2 is determined from salinity using the linear relationship of Fig. 5a and the atmospheric fCO_2 is chosen as the averaged value (353 μatm) measured over the area in 1996 (ETAMBOT 2). The fields of monthly mean CO_2 flux for April and September are shown in Fig. 9. As expected from SSS climatologies, the CO_2 sink area is confined along the coastline in spring, while it expands seaward between 5°N and 10°N in summer, under the influence of the NBC retroflection. The fluxes estimated from cruises data (Fig. 6) are in relatively good agreement with these monthly mean flux fields. The escaping flux of 2–3 mmol m^{-2} day^{-1} along 7.5°N (Leg B, ETAMBOT 2 in Fig. 6) is in the range (2–4 mmol m^{-2} day^{-1}) of the April mean field of CO_2 (Fig. 9). Nevertheless, this latter chart does not show the CO_2 sink occurred at 7.5°N, 35°W (end of Leg B and start of Leg C, Fig. 6, ETAMBOT 2). In September (Fig. 9, lower panel), the CO_2 sink north of 5°N, which extends eastwards with the advection of freshwater by the NECC, is more pronounced (< −2 mmol m^{-2} day^{-1}) than that estimated during ETAMBOT 1 (~ −0.5 mmol m^{-2} day^{-1}, Fig. 6). On the continental shelf (Fig. 6, bottom), the range (−10 to −40 mmol m^{-2} day^{-1}) of CO_2 flux measured during SABORD (May) is in good agreement with the lowest mean values indicated along the coast in April (< −20 mmol m^{-2} day^{-1}, Fig. 9). The monthly mean CO_2 flux at the air–sea interface calculated according to both L& M86 and Wkf92 parameterizations over the area

[1] Server: http://ferret.wrc.noaa.gov/fbin/climate.

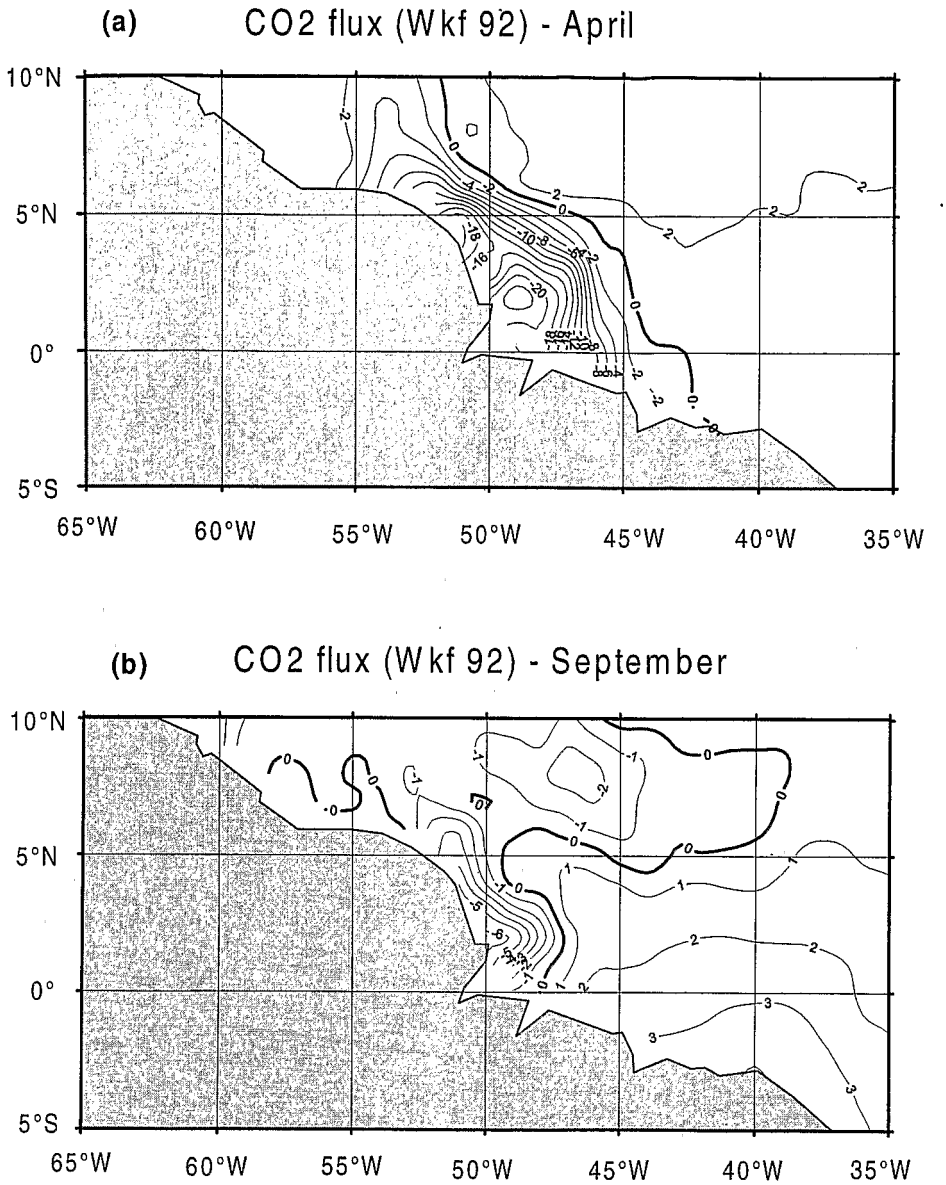

Fig. 9. Distribution of monthly mean CO_2 fluxes at the air–sea interface calculated from climatological fields of SST, wind velocity and SSS, according to the parameterization of Wkf92 (see text for the calculation method): (a) in April and (b) in September.

(5°S–10°N, 65°W–35°W) is shown in the Fig. 10d. On an annual average, the variabilities of monthly mean CO_2 flux and salinity are quite similar (Fig. 10b) and exhibit minima in April–June and maxima in December. The amplitude of the annual CO_2 flux variations reaches 2 mmol m^{-2} day^{-1}, according to the Wkf92 parameterization: the monthly CO_2 fluxes range from -1.0 mmol m^{-2} day^{-1} in April to 1.0 mmol m^{-2} day^{-1} in December. The net annual mean CO_2 flux in the area 5°S–10°N, 65°W–35°W does not significantly differ from zero: 0.08 ± 0.37 mmol m^{-2} day^{-1} using the L&M86 relationships and 0.12 ± 0.57 mmol m^{-2} day^{-1} with the Wkf92 relationships. This result can be compared with the

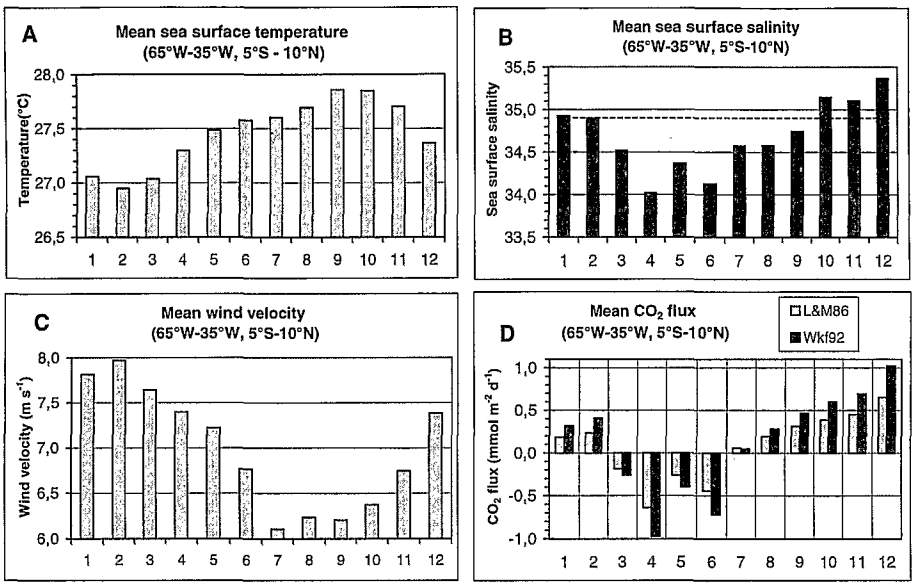

Fig. 10. Temporal diagrams of (A) monthly mean sea surface temperature, (B) monthly mean sea surface salinity, (C) monthly mean wind velocity, and (D) monthly mean CO_2 fluxes at the air–sea interface, over the area (5°S–10°N, 65°W–35°W). CO_2 fluxes are calculated from climatological fields (1977–1997) according to the parameterizations of L&M86 and Wkf92. The horizontal dashed line on the panel B indicates the salinity value (34.9) for which the oceanic CO_2 fugacity is equal to the atmospheric CO_2 fugacity (353 μatm) and the CO_2 flux goes to zero.

previous estimate of the annually mean CO_2 flux escaping from the Atlantic equatorial belt (5°S–5°N) between 35°W and 4°W from FOCAL cruises (Andrié et al., 1986) of 1.05 mmol m^{-2} day^{-1}, according to the L&M86 gas transfer–wind speed relationship. This clearly shows the role of river outflow (Amazon and secondarily Orinoco, the fourth most important river in the world) on CO_2 fluxes at the air–sea interface in the tropical Atlantic ocean. On an annual mean, the net source for atmospheric CO_2 observed in the central and eastern regions virtually disappears in the western part of the equatorial belt, where the fCO_2 level is lowered by rivers discharge.

6. Conclusions

The measurements of CO_2 fugacity at the air–sea interface in the western equatorial Atlantic ocean clearly shows that the area cannot be regarded as a source for atmospheric CO_2, in contrast to the central and eastern parts of the equatorial belt. Rivers run-off, primarily from the Amazon River, and secondarily from the Orinoco River, contribute to the decrease of oceanic fCO_2 by the dilution effect caused by the large input of freshwater. Fertilization of oceanic waters by river outflow enhances the biological pump of CO_2, which contributes up to 30% to the lowering of fCO_2 in these areas. In spite of the large approximations, and of the uncertainties that remains in the CO_2 flux calculation, our study clearly highlights the role of freshwater inputs to the ocean in the global CO_2 budget.

Acknowledgements

This research was supported by the Institut de Recherche pour le Développement (IRD), previously Institut Français de Recherche Scientifique pour le Développement en Coopération (ORSTOM). The ETAMBOT cruises are a contribution to WOCE, through the French Programme National d'Etude de la Dynamique du Climat (PNEDC). The authors

gratefully acknowledge the captains and crews of the R/V LE NOROIT, EDWIN LINK, and ANTEA, for their help and support. We thank Y. Gouriou, Chief Scientist of the ETAMBOT cruises, and scientists for their help in the data acquisition (J.M. Boré and B. Bourlès for implementation of Rosette/CTD probe and F. Baurand for nutrient measurements). The numerous and detailed comments of R. Wanninkhof and another anonymous reviewer led to a significant improvement of the manuscript.

References

Andrié, C., Oudot, C., Genthon, C., Merlivat, L., 1986. CO_2 fluxes in the tropical Atlantic during FOCAL cruises. J. Geophys. Res. 91, 11741–11755.

Bakker, D.C.E., de Baar, H.J.W., de Wilde, H.P.J., 1996. Dissolved carbon dioxide in Dutch coastal waters. Mar. Chem. 55, 247–263.

Bakker, D.C.E., de Baar, H.J.W., Bathmann, U.V., 1997. Changes of carbon dioxide in surface waters during spring in the Southern Ocean. Deep Sea Res., Part II 44, 91–127.

Baurand, F., Oudot, C., 1997a. Mesures des sels nutritifs. In: Recueil, D.D. (Ed.), Campagne, ETAMBOT 1. Vol. 2: Traceurs géochimiques. Doc. Sci. Centre ORSTOM Cayenne, No. O.P. 23, 27–58.

Baurand, F., Oudot, C., 1997b. Mesures des sels nutritifs. In: Recueil, D.D. (Ed.), Campagne ETAMBOT 2. Vol. 2: Traceurs géochimiques. Doc. Sci. Centre ORSTOM Cayenne, No. O.P. 25, 35–75.

Bourlès, B., Marin, F., 1997. Mesures In: Recueil, D.D. (Ed.), Campagne ETAMBOT 2. Vol.1: Introduction — Mesures 'en route' — Courantométrie ADCP — Mesures $CTDO_2$ — Coupes de distributions verticales. Doc. Sci. Centre ORSTOM Cayenne, No. O.P. 24, 19–40.

Bourlès, B., Molinari, R.L., Johns, E., Wilson, W.D., Leaman, K.D., 1999. Upper layer currents in the Western Tropical North Atlantic (1989–1991). J. Geophys. Res. 104, 1361–1375.

Brewer, P.G., Goldman, J.C., 1976. Alkalinity changes generated by phytoplankton growth. Limnol. Oceanogr. 21, 108–117.

Broecker, W.S., Peng, T.H., 1982. Tracers in the sea. Eldigio, Palisades, NY, 690 pp.

Broecker, H.C., Siems, W., 1984. The role of bubbles for gas transfer from water to air at higher windspeeds. Experiments in the wind-wave facility in Hamburg. In: Brutsaert, W., Jirka, G.H. (Eds.) Gas transfer at water surfaces. Reidel, Dordrecht, Holland, pp. 229–236.

Brzezinski, M.A., 1985. The Si:C:N ratio of marine diatoms: interspecific variability and the effect of some environmental variables. J. Phycol. 21, 347–357.

Cadee, G.C., 1975. Primary production off the Guyana coast. Neth. J. Sea Res. 9, 128–143.

Chen, C.T.A., 1993. Carbonate chemistry of the wintertime Bering Sea marginal ice zone. Cont. Shelf Res. 13, 67–87.

Copin-Montegut, C., 1989. A new formula for the effect of temperature on the partial pressure of CO_2 in seawater. Mar. Chem. 27, 143–144.

DeMaster, D.J., Pope, R.H., 1996. Nutrient dynamics in Amazon shelf waters: results from AMASSEDS. Cont. Shelf Res. 16, 263–289.

DeMaster, D.J., Smith, W.O. Jr., Nelson, D.M., Aller, J.Y., 1996. Biogeochemical processes in Amazon shelf waters: chemical distributions and uptake rates of silicon, carbon and nitrogen. Cont. Shelf Res. 16, 617–643.

Dessier, A., Donguy, J.R., 1994. The sea surface salinity in the tropical Atlantic between 10°S and 30°N — seasonal and interannual variations (1977–1989). Deep-Sea Res. 41, 81–100.

Dickson, A.G., 1990. Thermodynamics of the dissociation of boric acid in synthetic seawater from 273.15 to 298.15 K. Deep-Sea Res. 37, 755–766.

Dickson, A.G., 1993. pH buffers for seawater media based on the total hydrogen ion concentration scale. Deep-Sea Res. 40, 107–118.

Dorman, C.E., Bourke, R.H., 1981. Precipitation over the Atlantic ocean, 30°S to 70°N. Mon. Weather Rev. 109, 554–563.

Frankignoulle, M., Bourge, I., Canon, C., Dauby, P., 1996. Distribution of surface seawater partial CO_2 pressure in the English Channel and in the Southern Bight of the North Sea. Cont. Shelf Res. 16, 381–395.

Froelich, P.N. Jr., Atwood, D.N., Giese, G.S., 1978. Influence of Amazon River discharge on surface salinity and dissolved silicate concentration in the Caribbean sea. Deep Sea Res. 25, 735–744.

Gouriou, Y., 1997a. Calibration des mesures $CTDO_2$. In: Recueil D.D. (Ed.), Campagne ETAMBOT 1. Vol. 1: Introduction — Mesures 'en route' — Courantométrie ADCP — Mesures $CTDO_2$ — Coupes de distributions verticales. Doc. Sci. Centre ORSTOM Cayenne, No. O.P. 22, 125–168.

Gouriou, Y., 1997b. Calibration des mesures $CTDO_2$. In: Recueil D.D. (Ed.), Campagne ETAMBOT 2. Vol. 1: Introduction — Mesures 'en route' — Courantométrie ADCP — Mesures $CTDO_2$ — Coupes de distributions verticales. Doc. Sci. Centre ORSTOM Cayenne, No. O.P. 24, 159-186.

Goyet, C., Adams, R., Eischeid, G., 1998a. Observations of the CO_2 system properties in the tropical Atlantic Ocean. Mar. Chem. 60, 49–61.

Goyet, C., Millero, F.J., O'Sullivan, D.W., Eischeid, G., McCue, S.J., Bellerby, R.G.J., 1998b. Temporal variations of pCO_2 in surface seawater of the Arabian Sea in 1995. Deep-Sea Res., Part I 45, 609–623.

Haines, M.A., Luther, M.E., Fine, R.A., 1997. Model-validated parameterization for air–sea gas transfer in the north Indian Ocean. Geophys. Res. Lett. 24, 2545–2548.

Keeling, C.D., Waterman, L.S., 1968. Carbon dioxide in surface ocean waters: 3. Measurements on Lusiad Expedition 1962–1963. J. Geophys. Res. 73, 4529–4541.

Kempe, S., Pegler, K., 1991. Sinks and sources of CO_2 in coastal seas: the North Sea. Tellus 43B, 224–235.

Key, R.M., Stallard, R.F., Moore, W.S., Sarmiento, J.L., 1985. Distribution of Ra-226 and Ra-228 in the Amazon River estuary. J. Geophys. Res. 90, 6995–7004.

Kumar, M.D., Naqvi, S.W.A., George, M.D., Jayakumar, D.A., 1996. A sink for atmospheric carbon dioxide in the northeast Indian ocean. J. Geophys. Res. 101, 18121–18125.

Lefèvre, N., Moore, G., Aiken, J., Watson, A., Cooper, D., Link, R., 1998. Variability of pCO_2 in the tropical Atlantic in 1995. J. Geophys. Res. 103, 5623–5634.

Lentz, S.J., 1995. Seasonal variations in the horizontal structure of the Amazon Plume inferred from historical hydrographic data. J. Geophys. Res. 100, 2391–2400.

Lentz, S.J., Limeburner, R., 1995. The Amazon River Plume during AMASSEDS: spatial characteristics and salinity variability. J. Geophys. Res. 100, 2355–2375.

Limeburner, R., Beardsley, R.C., Soares, I.D., Lentz, S.J., Candela, J., 1995. Lagrangian flow observations of the Amazon River discharge into the North Atlantic. J. Geophys. Res. 100, 2401–2415.

Liss, P., Merlivat, L., 1986. Air–sea gas exchange rates: introduction and synthesis. In: Buat-Ménard, P. et al. (Ed.), The Role of Air–Sea Exchange in Geochemical Cycling. Reidel, Hingham, MA, pp. 113–127.

Marin, F., 1997. Mesures météorologiques. In: Recueil D.D.(Ed.), Campagne ETAMBOT 1. Vol. 1: Introduction — Mesures 'en route' — Courantométrie ADCP — Mesures $CTDO_2$ — Coupes de distributions verticales. Doc. Sci. Centre ORSTOM Cayenne, No. O.P. 22, 18–29.

McNeil, C.L., Merlivat, L., 1996. The warm oceanic surface layer: implications for CO_2 fluxes and surface gas measurements. Geophys. Res. Lett. 23, 3575–3578.

Millero, F.J., 1995. Thermodynamics of the carbonate system in the oceans. Geochim. Cosmochim. Acta 59, 661–677.

Muller-Karger, F.E., Mc Clain, C.R., Richardson, P.L., 1988. The dispersal of the Amazon's water. Nature 333, 56–59.

Mullin, J.B., Riley, J.P., 1955. The spectrophotometric determination of silicate–silicon in natural waters with special reference to sea water. Anal. Chim. Acta 12, 162–170.

Neumann, G., 1969. Seasonal salinity variations in the upper strata of the western tropical Atlantic ocean: 1. Sea surface salinities. Deep Sea Res. 16, 165–177, suppl.

Olsson, K., Anderson, L.G., 1997. Input and biogeochemical transformation of dissolved carbon in the Siberian shelf seas. Cont. Shelf Res. 17, 819–833.

Oudot, C., Andrié, C., Montel, Y., 1987. Evolution of oceanic and atmospheric CO_2 over the 1982–1984 period in tropical Atlantic (in French). Deep Sea Res. 34, 1107–1137.

Oudot, C., Ternon, J.F., Lecomte, J., 1995. Measurements of atmospheric and oceanic CO_2 in the tropical Atlantic: 10 years after the 1982–1984 FOCAL cruises. Tellus 47B, 70–85.

Pailler, K., Bourlès, B., Gouriou, Y., 1999. The barrier layer in the western tropical Atlantic ocean. Geophys. Res. Let. 26, 2069–2072.

Perry, G.D., Duffy, P.B., Miller, N.L., 1996. An extended data set of river discharges for validation of general circulation models. J. Geophys. Res. 101, 21339–21349.

Richardson, P.L., Reverdin, G., 1987. Seasonal cycle of velocity in the Atlantic North Equatorial Countercurrent as measured by surface drifters current meters and ship drift. J. Geophys. Res. 92, 3691–3708.

Richardson, P.L., Hufford, G.E., Limeburner, R., Brown, W.S., 1994. North Brazil Current retroflection eddies. J. Geophys. Res. 99, 5081–5093.

Richey, J.E., Hedges, J.I., Devol, A.H., Quay, P.D., Victoria, R., Martinelli, L., Forsberg, B.R., 1990. Biogeochemistry of carbon in the Amazon River. Limnol. Oceanogr. 35, 352–371.

Richey, J.E., Victoria, R.L., Salati, E., Forsberg, B.R., 1991. The biogeochemistry of a major river system: the Amazon case study. In: Degens, E.T., Kempe, S., Richey, J.E. (Ed.), Biogeochemistry of Major World Rivers, Scope 42, pp. 57–74.

Robertson, J.E., Watson, A.J., 1992. Thermal skin effect of the surface ocean and its implications for CO_2 uptake. Nature 358, 738–740.

Roos, M., Gravenhorst, G., 1984. The increase in oceanic carbon dioxide and the net CO_2 flux into the north Atlantic. J. Geophys. Res. 89, 8181–8193.

Roy, R.N., Roy, L.N., Vogel, K.M., Porter-Moore, C., Pearson, T., Good, C.E., Millero, F.J., Campbell, D.M., 1993. The dissociation constants of carbonic acid in seawater at salinities 5 to 45 and temperatures 0 to 45°C. Mar. Chem. 44, 249–267.

Schneider, B., Morlang, J., 1995. Distribution of the CO_2 partial pressure in the Atlantic ocean between Iceland and the Antarctic peninsula. Tellus 47B, 93–102.

Servain, J., Seva, M., Lukas, S., Rougier, G., 1987. Climatic Atlas of the tropical Atlantic wind stress and sea surface temperature: 1980–1984. Ocean–Air Inter. 1, 109–182.

Skirrow, G., 1975. The dissolved gases–carbon dioxide. In: Riley, J.P., Skirrow, G. (Ed.), Chemical Oceanography. Academic Press, London, Vol. 2, pp. 1–192.

Smethie, W.M. Jr., Takahashi, T., Chipman, D.W., Ledwell, J.R., 1985. Gas exchange and CO_2 flux in the tropical Atlantic ocean determined from ^{222}Rn and pCO_2 measurements. J. Geophys. Res. 90, 7005–7022.

Smith, W.O. Jr., DeMaster, D.J., 1996. Phytoplankton biomass and productivity in the Amazon River plume: correlation with seasonal river discharge. Cont. Shelf Res. 16, 291–319.

Takahashi, T., Prince, L.A., Broecker, W.S., Bainbridge, A.E., 1978. Carbon dioxide in the surface waters of the Atlantic and Pacific oceans (abstract). Trans. EOS AGU 59, 1102.

Takahashi, T., Olafsson, J., Goddard, J.G., Chipman, D.W., Sutherland, S.C., 1993. Seasonal variation of CO_2 and nutrients in the high-latitude surface oceans: a comparative study. Global Biogeochem. Cycles 7, 843–878.

Tans, P.P., Fung, I.Y., Takahashi, T., 1990. Observational constraints on the global atmospheric CO_2-budget. Science 247, 1431–1438.

UNESCO, 1987. Thermodynamics of the carbon dioxide system in seawater. Report by the carbon dioxide sub-panel of the joint panel on oceanographic tables and standards. UNESCO technical papers in marine science, Vol. 51.

Van Scoy, K.A., Morris, K.P., Robertson, J.E., Watson, A.J., 1995. Thermal skin effect and the air–sea flux of carbon dioxide: A seasonal high-resolution estimate. Global Biogeochem. Cycles 9, 253–262.

Wanninkhof, R.H., 1992. Relationship between wind speed and gas exchange over the ocean. J. Geophys. Res. 97, 7373–7382.

Watson, A.J., Upstill-Goddard, R.C., Liss, P.S., 1991. Air–sea gas exchange in rough and stormy seas measured by a dual-tracer technique. Nature 349, 145–147.

Weiss, R.F., 1974. Carbon dioxide in water and seawater: the solubility of a non-ideal gas. Mar. Chem. 2, 203–215.

Weiss, R.F., Price, B.A., 1980. Nitrous oxide solubility in water and seawater. Mar. Chem. 8, 347–359.

Yoo, J.M., Carton, J.A., 1990. Annual and interannual variations of the freshwater budget in the Tropical Atlantic Ocean and the Caribbean Sea. J. Phys. Oceanogr. 20, 831–845.

USA mailing notice: *Marine Chemistry* (ISSN 0304-4203) is published monthly by Elsevier Science B.V. (P.O. Box 211, 1000 AE Amsterdam, The Netherlands). Annual subscription price in the USA is US $1565 (valid in North, Central and South America), including air speed delivery. Periodical postage rate paid at Jamaica, NY 11431.
USA POSTMASTER: Send address changes to *Marine Chemistry*, Publications Expediting Inc., 200 Meacham Ave, Elmont, NY 11003.
AIRFREIGHT AND MAILING in the USA by Publications Expediting Inc., 200 Meacham Avenue, Elmont, NY 11003.

Notes to Contributors
A detailed *Guide for Authors* is available upon request or from the Marine Chemistry Home Page at: http//:www.elsevier.nl/locate/Marchem. Please pay special attention to the following notes:

Language
The official language of the journal is English.

Preparation of the text
(a) The manuscript should preferably be prepared on a word processor and printed with double spacing and wide margins and include an abstract of not more than 500 words. Please provide up to six subject keywords (at least four of which should be selected from the *Aquatic Science & Fisheries Thesaurus*), plus regional index terms. The metric system should be used throughout.
(b) The title page should include: the title, the name(s) of the author(s), their affiliations, fax and e-mail numbers. In case of more than one author, please indicate to whom the correspondence should be addressed.

References
(a) All references cited in the text are to be listed at the end of the paper.
(b) In the text refer to the author's name (without initials) and year of publication.
(c) References in the text should be arranged chronologically. The list of references should be arranged alphabetically by authors' names, and chronologically per author.
(d) Full details are to be found in the Guide for Authors on the journal's website.

Tables
Tables should be compiled on separate sheets and should be numbered according to their sequence in the text.

Illustrations
(a) All illustrations should be numbered consecutively and referred to in the text.
(b) Drawings should be completely annotated, the size of the lettering being appropriate to that of the drawings, but taking into account the possible need for reduction in size (preferably not more than 50%). The page format of *Marine Chemistry* should be considered in designing the drawings.
(c) Photographs must be of good quality, printed on glossy paper.
(d) Figure captions should be supplied on a separate sheet.
(e) Colour figures can be accepted providing the reproduction costs are met by the author. Please consult the publisher for further information.

Proofs
One set of proofs will be sent to the corresponding author, to be checked for typesetting/editing. The author is not expected to make changes or corrections that contstitute departures form the article in its accepted form. Proofs should be returned within 3 days as far as possible. Arrangements should be made with colleagues for proofs to be checked in the author's absence.

Reprints
Fifty reprints of each article published are supplied free of charge. Additional reprints can be ordered on a reprint order form, which will be sent to the first author upon acceptance of the article.

Submission of manuscripts
Five copies should be submitted to: Editorial Office *Marine Chemistry*, RSMAS, MAC, University of Miami, 4600 Rickenbacker Causeway, FL 33149-1098, USA. The indication of a fax and e-mail number on submission of the manuscript could assist in speeding communications. Illustrations should also be submitted in five copies: one set should be in a form ready for reproduction; the other four may be of lower quality. Authors are requested to submit, with their manuscripts, the names and full addresses (plus fax numbers if possible) of four potential referees.

Submission of electronic text
Elsevier Science is now publishing all manuscripts using electronic production methods, and therefore needs to receive the electronic files of your article with the hardcopy of the accepted version. Below are some general points to enable us to use your files. Always supply high quality originals of your artwork with the hardcopy of the manuscript, as we cannot guarantee the usability of electronic graphic files. Electronic files can be submitted on 3.5" diskette, CD or Zip-disk. Please name your files using the correct software extension, e.g. text.doc, tbl-5.xls, fig1.cdr, fig1a.eps, fig1.jpg, etc. In case of illustrations please give the resolution and also indicate if the data have been scanned. Save text on a separate disk from the graphics. Label all disks with your name, journal title, software (e.g. Word 7, Adobe Illustrator 6.0), compression software if used, hardware used (e.g. IBM [compatible], Mac) and file names. It is essential that the electronic and hardcopy versions are **identical**. The hardcopy will be used as the definitive version of the article. Further details about electronic submission can be found in the Guide for Authors on the journal's website.

Authors in Japan please note: Upon request, Elsevier Science K.K. will provide authors with a list of people who can check and improve the English of their paper (*before submission*). Please contact our Tokyo office: Elsevier Science K.K., 1-9-15 Higashi Azabu, Minato-ku, Tokyo 106-0044; Tel. +81 3 5561 5032; Fax +81 3 5561 5045.

Submission of an article is understood to imply that the article is original and unpublished and is not being considered for publication elsewhere. Upon acceptance of an article by the journal, the author(s) will be asked to transfer the copyright of the article to the publisher. This transfer will ensure the widest possible dissemination of information. The author is responsible for obtaining permission to use any copyrighted material.

Ocean Energies

Environmental, Economic and Technological Aspects of Alternative Power Sources

by R.H. Charlier *and* J.R. Justus

Elsevier Oceanography Series Volume 56

This timely volume provides a comprehensive review of current technology for all ocean energies. It opens with an analysis of ocean thermal energy conversion (OTEC), with and without the use of an intermediate fluid. The historical and economic background is reviewed, and the geographical areas in which this energy could be utilized are pinpointed. The production of hydrogen as a side product, and environmental consequences of OTEC plants are looked at. The competitiveness of OTEC with conventional sources of energy is analysed. Optimisation, current research and development potential are also examined.

Each chapter contains bibliographic references. The author has also distinguished between energy schemes which might be valuable in less-industrialized regions of the world, but uneconomical in the developed countries. A large number of illustrations support the text.

Every effort has been made to ensure that the book is readable and accessible for the specialist as well as the non-expert. It will be of particular interest to energy economists, engineers, geologists and oceanographers, and to environmentalists and environmental engineers.

Short Contents: .

A complete list of contents is available from the publisher.

1993 556 pages
Dfl. 390.00 (US $ 222.75)
ISBN 0-444-88248-0

ELSEVIER SCIENCE B.V.
P.O. Box 1930
1000 BX Amsterdam
The Netherlands

P.O. Box 945
Madison Square Station
New York, NY 10160-0757

The Dutch Guilder (Dfl.) prices quoted apply worldwide. US $ prices quoted may be subject to exchange rate fluctuations. Customers in the European Community should add the appropriate VAT rate applicable in their country to the price.

ELSEVIER SCIENCE B.V.